

**An Analysis of Refractivity Ducting  
During the July 2002 R/V Pt Sur  
SoCal Underway Period**

**John Daziens**

**OC 3570**

**Operational Oceanography/Meteorology**

**Professor Curtis Collins**

**Professor Peter Guest**

**19 September 2002**

## Project Definition

The scope of this project was to analyze the elevated and surface ducting conditions present during the OC3570 underway period. The propagation path changes between elevated and surface duct conditions would then be determined using the Advanced Refractive Effects Prediction System (AREPS), and the factors leading to these ducting conditions.

Following the initial data analysis, this project scope was amended to analyze the lowest elevated duct characteristics.

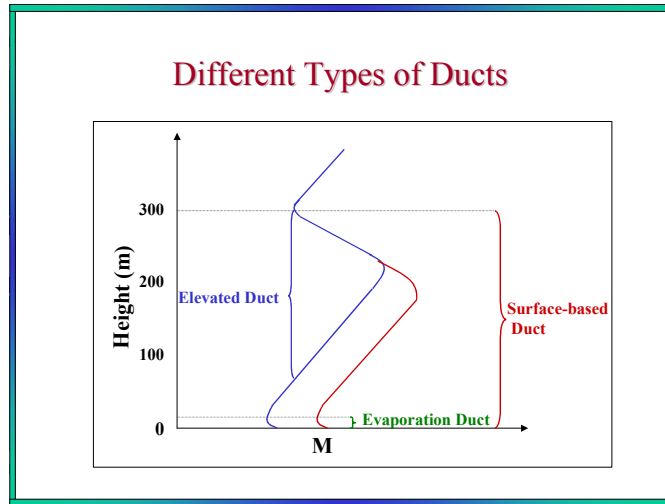


Fig 1: Duct Types

## Introduction

Ducting conditions distort the propagation paths of electromagnetic (EM) emissions. The extended ranges experienced by trapped energy provide an opportunity for greater communication and target detection if properly exploited. Additionally, effects such as shadow zones are also produced by the refractive conditions. Fleet assets therefore need proper prediction of current refractive conditions to maximize advantages and minimize or mitigate any coverage gaps.

Refractivity is a function of atmospheric temperature and vapor pressure. The gradient of refractivity determines the presence of ducting conditions:

$$N = 77.6 P/T + (3.73 \times 10^5) e/T$$

Where  $P$  is the pressure and  $e$  is the vapor pressure, both in millibars, and  $T$  is the Temperature in degrees Celsius. For convenience, a modified measure of refractivity is often used:

$$M = N + 0.157 h$$

This function of  $N$  and height,  $h$  (meters), indicates ducting conditions in negative  $M$ -gradient regions. Trapping of emissions is dependent upon the wavelength (or frequency) of the EM energy.

$$f_{\min} \cong \left[ 3.6 \cdot 10^5 \text{ MHz} / m^{-3/2} \right] d^{-3/2}$$

Minimum Trapped Frequency (MHz)	Maximum Trapped Wavelength	Radar (Radio) Band	Duct Thickness	
			feet	meters
150	2.0 m	A (VHF)	587	179.0
192	1.56 m	A (VHF)	499	152.0
220	1.36 m	A (TAC UHF)	453	138.0
425	70.6 cm	B (TAC UHF)	294	89.6
1000	30.0 cm	D	166	50.6
3000	10.0 cm	F	80	24.3
5800	5.2 cm	G	51	15.6
8500	3.5 cm	I	40	12.2
9600	3.1 cm	I	37	11.2
10250	2.9 cm	J	35	10.7
15000	2.0 cm	J	27	8.3
30000	1.0 cm	K	17	5.24

Fig 2: Trapping Frequencies

Battlegroups conduct only limited measuring of refractive conditions throughout the day. Upper air observations using balloon launches are generally performed only once per day. Other measurement methods such as Refractivity From Clutter (RFC) are still in the experimental stages and not yet deployed for Fleet use. Frequent atmospheric measurements are critical to detecting low-level ducting conditions. Evaporative and surface duct changes can vary quickly with changes in temperature and humidity profiles throughout the day.

### Procedure

All Rawindsonde balloon data was evaluated for refractive conditions. Data sets included full upper air profiles and “up-down” launches – an observation of approximately the lower 2000 meters of the atmosphere through the use of a gas release nozzle (i.e. drilled syringe) attached to the helium balloon. The MATLAB program “m\_n\_profile” attached as an enclosure was used to calculate and plot the M and N values versus height. Twenty-one Rawindsonde data files were then analyzed for ducting conditions.

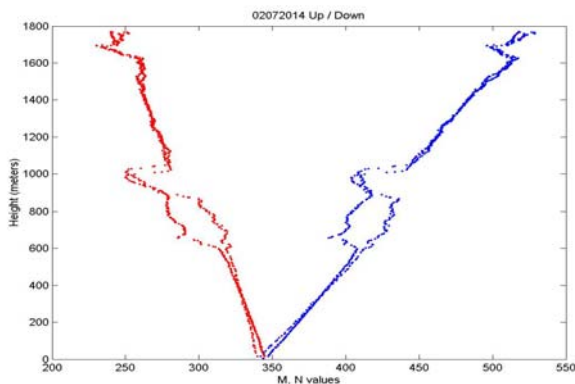


Fig 3a, 3b: Sample Rawindsonde M (blue), N (red) profile from balloon data

Phase two of the data analysis focused solely on the lowest elevated duct. Inversion and duct height discrepancies were clearly present between the “up” and “down” legs of the soundings. These errors are largely due to the effects of moisture upon the travelling sensor when passing through cloud layers. A detailed explanation of the sensor error cause and effect is the subject of an additional class project and beyond the scope of this paper (see Newton, 2002 project for details). However, to eliminate the noise and smooth the elevated duct analysis, only the downward portion of the “up down” and upper air soundings (when available) were used. Fourteen Rawindsonde data files were then analyzed using the MATLAB “m\_n\_down” program (see enclosures). The resulting plots were consolidated into time series of elevated duct height and thickness.

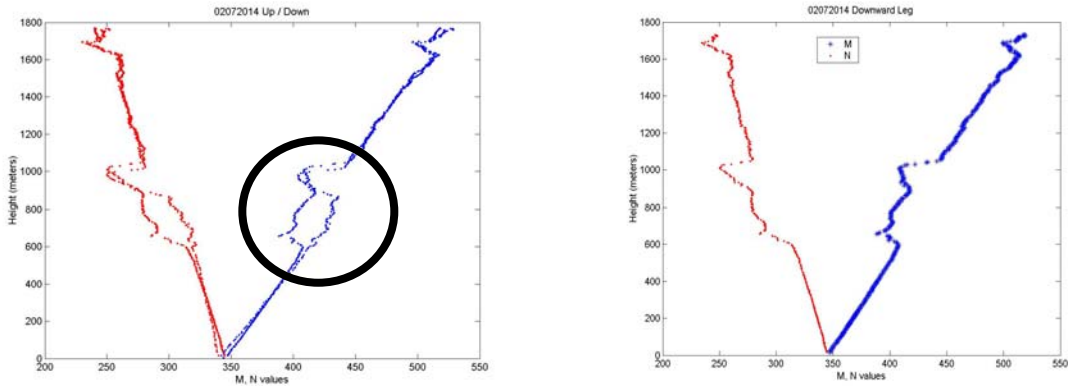


Fig 4a, 4b: Sample Rawindsonde “Up/Down” processed into downward leg only

## Results

No evaporative or surface ducts were found in the Rawindsonde observations. Launches took place throughout the transit from Monterey to the southern California operating area, and at well sampled times periods. Neither the location nor the temporal launch time changes detected any low level ducting using the Rawindsonde data.

Elevated ducts were present throughout the cruise. The lowest elevated duct height varied as follows:

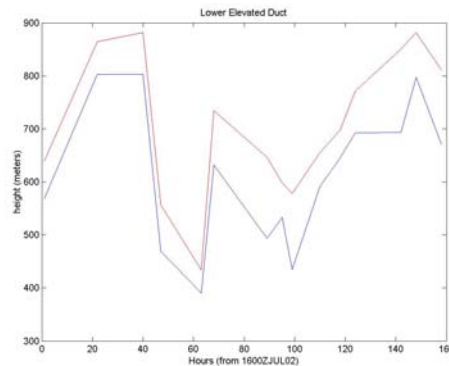


Fig 5: Lowest Elevated Duct Height (time from 0100 16July – 1400 22July)

Duct thickness trends were also calculated for the cruise period:

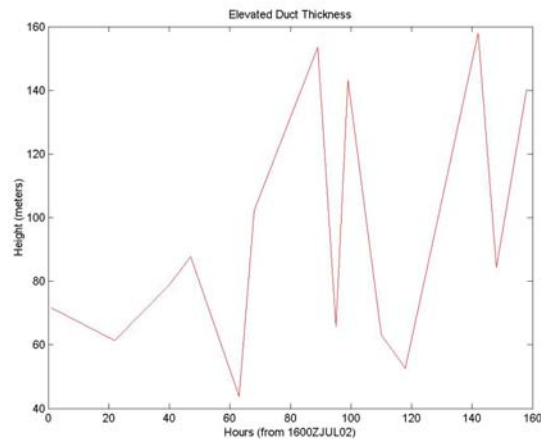


Fig 6: Lowest elevated duct thickness trend

### Discussion

A large drop in the elevated duct height is seen between the 16-17 July observations and 18 July. Following departure from Monterey, the Pt Sur encountered elevated ducts at approximately 800 meters. The 16 July 2200Z, and 17 July 0600Z and 1600Z all show the high, thin layer. As the vessel moved eastward towards the California shore, the layer moved lower and grew in thickness. Sea level pressure, sea surface temperature, the temperature/dew point spread, and long wave and shortwave irradiance are all consistent during this time period. Of note, the sea surface temperatures encountered in this region on 18 July (approximately 14 degrees Celsius) were indicative of upwelling areas. Colder sea surface temperatures created a less humid boundary layer and cooler boundary layer, reducing the strength of entrainment mixing, and therefore contributed to the lowering of the inversion and duct. (Davidson, 2002)

Also the soundings on 17 July 2300Z and 18 July 1500Z were taken approximately 60 miles inland of the earlier observations. An earlier project by (ENS Doric, 2001) observed the variance of the marine boundary layer thickness relative to longitudinal changes from the coast. (Given this operational cruise destination in the vicinity of the San Clemente, Santa Cruz, and other southern California islands, this "distance from shore" trend was not analyzed).

A rapid rise in elevated duct height was also observed later on 18 July. Following the duct height minimum elevation at the 1500Z sounding, the duct height rose over 200 meters within five hours. Ship position remained within ten kilometers of initial position during this period. This sudden rise corresponded with the short-term clearing and mesoscale eddy event encountered throughout the evening of 18-19 July. Increased shortwave radiation (solar heating), decreased sea surface temperature, decreased sea surface pressure, and significant reduction of longwave radiation are all evident during this period. Analysis of specific features driving this eddy-clearing event are covered in-depth by another student project, and are beyond the scope of this paper (see Beattie, 2002 project for more details).

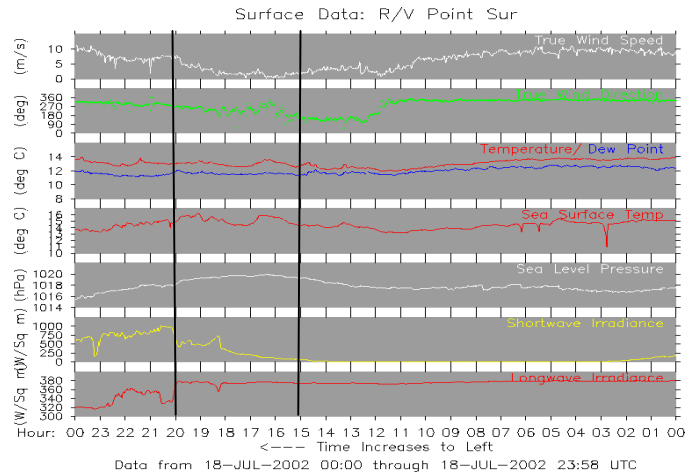
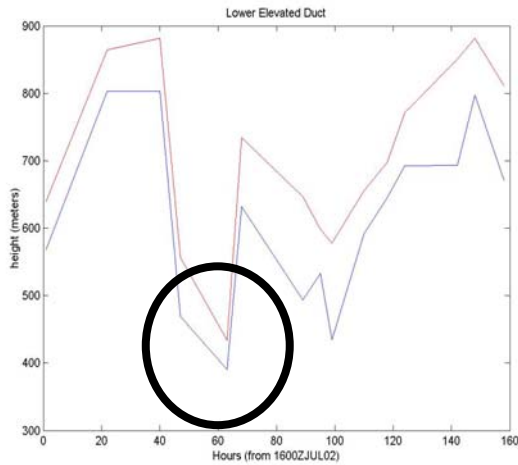


Fig 7a, 7b: Duct height minimum at 1500Z 18July (marked on Fig 7a) and rise at 2000Z.

One other event of interest was the period of rising elevated ducts on 22 July towards the end of the time series. The duct height continued to rise following the 18 July minimum, suggestive of synoptic influences. From the local afternoon on 21 July (i.e. after 2000Z 21July), reduced longwave irradiance was recorded, along with an increased temperature-dew point spread. SLP increased drastically around 1500Z on 21 July, and hovered between 1026 and 1028 throughout this period. Sea surface temperatures remained in the 17-18 degree Celsius range, creating a relatively warm surface layer for this cruise. These observations and the observed clearing resulted from an upper level low moving into the region. The vertical motion associated with the upper level circulation led to the raising of the inversion layer and elevated duct. Further details of the event are the subject of a separate class project (see Okon, 2002 projects).

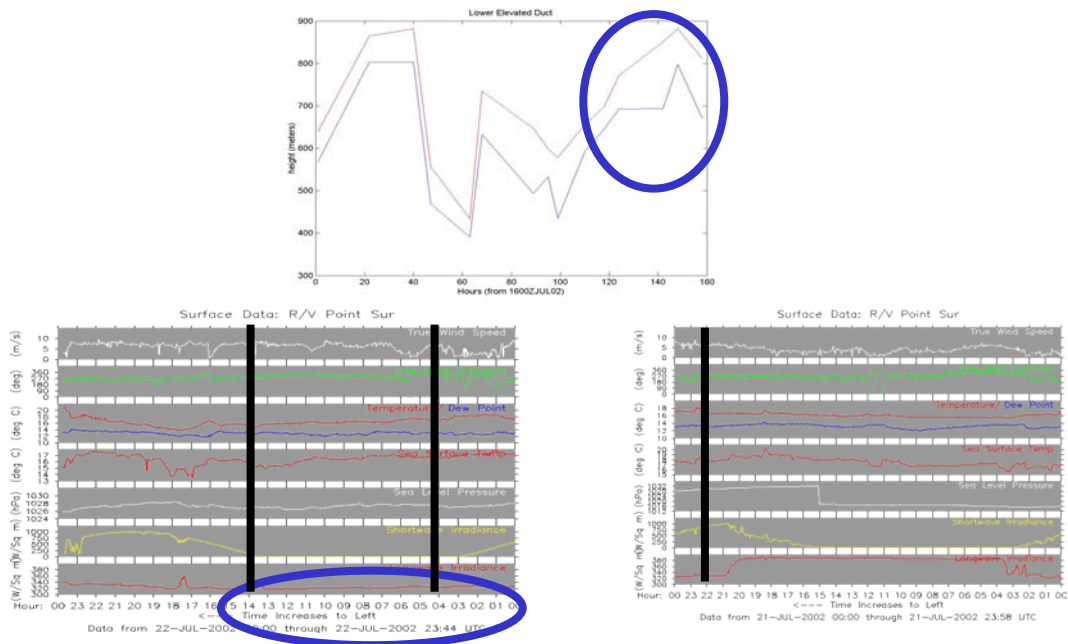


Fig 8a-c: Elevated duct height rise in response to an upper-level synoptic disturbance. Rawinsonde observation times are marked on surface observations, with 1400Z 22 July being the last data point for the time series.

## **Conclusions**

Surface ducting conditions were not found evident from the Rawindsonde analysis during this operational cruise. As such, no comparisons of AREPS propagation fields were performed. Instead, the project focus shifted to an analysis of the lowest elevated duct and factors affecting the changes in layer heights.

Synoptic and mesoscale events were the primary drivers for elevated duct height changes. Rising duct heights corresponded with the eddy and synoptic clearing events also analyzed for the cruise.

Large diurnal variances of the elevated duct heights were not observed from this data set.

A comparison to low-level “kite” Rawindsonde measurements indicated the rapid formation of surface duct conditions. Analysis of the 19 July “up/down” data yielded no surface duct. However, kite data taken only 2-3 hours after a balloon launch indicated a low level surface duct had formed. (See Kuehn, 2002 projects for further details).

## **WORKS CONSULTED**

Davidson, Kenneth L. "Estimation of Atmosphere Effects on Rf/EO propagation." MR4416, 2002.

Dorics, ENS Theodore. "Examining Spatial and Temporal Changes in Refractive Conditions." OC3570, Sep 01.

Miller, LCDR Henry A. "Evaluation of a Statistical Refractivity Model using Observations form R/V PT SUR." OC3570, Sep 2001.